THE PENNSYLVANIA STATE UNIVERSITY
SCHREYER HONORS COLLEGE

DEPARTMENTS OF BIOLOGY & PSYCHOLOGY

THE SALIENCE OF LOWER-ORDER FEATURES IN HIGHLY SELF-SIMILAR WALLPAPER GROUPS

SHIVAM VEDAK
SPRING 2014

A thesis
submitted in partial fulfillment
of the requirements
for a baccalaureate degree
in Biology
with interdisciplinary honors in Biology and Psychology

Reviewed and approved* by the following:

Rick Gilmore
Associate Professor of Psychology
Thesis Supervisor

Gong Chen
Professor of Biology
Honors Adviser

Rick Jacobs
Professor of Psychology
Honors Adviser

* Signatures are on file in the Schreyer Honors College.

ABSTRACT

There exists an abundance of visual symmetry within our environment. Yet research on human perception has almost exclusively been limited to studies of a single type of symmetry— two-fold reflection—leaving uncertainty about human perceptual sensitivity to the other types of symmetry as derived from the mathematics of Group Theory. Clarke et al. (2011) found that five of the seventeen wallpaper groups—P1, P3M1, P31M, P6, and P6M—have a high degree of self-similarity, as determined by the frequency with which participants grouped random-dot noise representations of the same wallpaper group together. The current study attempts to replicate Clarke et al. (2011) in a limited form. Here, we sought to understand the salience of lower-order features within each of five wallpaper groups, and concordantly, their impact on symmetry detection. Adult participants were presented with twenty exemplars of each of the five aforementioned wallpaper groups and instructed to sort them into as many subsets as they wished based on any criteria they saw appropriate. Participants were then surveyed on the methods they used to classify these images. Analysis suggest several factors—including contrast and presence of salient secondary structures—influence the detection of symmetry in wallpaper groups.

LIST OF FIGURES

ACKNOWLEDGEMENTS

I would like to thank Dr. Rick Gilmore for his guidance and support not only throughout the completion of this thesis, but over the last four years in his research lab. I would also like to thank Amanda Thomas and Olivia Reed for their assistance and guidance throughout the course of this project. Lastly, I would like to thank Dr. Gong Chen and Dr. Rick Jacobs for their commitment to me in their integral role as honors advisers.

Introduction

Background

Symmetry is pervasive in our visual environment. In the natural world, it can most easily be observed in flowers, the petals of which are often radially symmetrical, and in the bodies of vertebrate animals, which predominantly display bilateral symmetry across the midline of the body (Tyler, 1995). In the artificial environment, the prevalence of symmetry can at least partially be attributed to functional advantages; symmetric objects are usually well balanced, and are often easier for humans to interact with due to our inherent anatomical symmetry (Treder, 2010). However, the ubiquity of symmetry in art and architecture indicates a purpose beyond mere functionality—aesthetic appeal. Indeed, historical records illustrate a human fascination with symmetrical forms since the earliest instances of art and architecture, including the centered mass-distribution of the Mayan pyramids and repeating patterns found on Persian rugs (Tyler, 2000).

While the exact reason for the aesthetic appeal of symmetry is unknown, it can be argued that it is derived from perceptual specializations developed in response to the variance of symmetry in the natural environment. Since inanimate natural objects, which predominantly consist rocks and geological formations, do not generally exhibit any forms of symmetry, the presence of symmetry usually betrays the presence of living organisms (Tyler, 1995). Thus, the development of symmetry detection mechanisms within the perceptual system possibly conferred an evolutionary advantage (Tyler, 2000). Indeed, there is consensus among the literature that symmetry detection is a fundamental property of the human visual system (Swaddle, 1999), and that it is an automatic process applied to all visual input (Treder, 2010). Moreover, this process has been demonstrated to occur very quickly—within 100 milliseconds of image presentation (Treder, 2010). However, despite the established importance of symmetry detection within the human visual system, the vast majority of research in this realm has been limited to reflectional (i.e. mirror) symmetry, leaving uncertainty about human perceptual sensitivity to the other types.

Atomic Geometrical Symmetries, Isometries, and Wallpaper Groups

Geometrical symmetry in two- and three-dimensional patterns has been studied mathematically. An image is considered to have geometrical symmetry if it contains a transformation of a structure within the Euclidean (i.e. two- or three-dimensional) plane such that it preserves the overall geometric properties of the structure (e.g. size, shape) (Weyl, 1952). Such a transformation is termed an *isometry*. There are four forms of atomic geometrical symmetries in two-dimensional Euclidean space, derived from the four possible (and identically named) isometries. (i) Reflection is the inversion of the structure with respect to the plane, so that each element is transferred perpendicularly through the plane to a point the same distance the other side of it. (ii) Rotation is circular transformation of the structure around a fixed point by a certain angle. (iii) Translation is the movement of every point of the structure by the same amount in a given direction, with no alteration of orientation. (iv) Glide reflection is a transformation that is a combination of a reflection across a line and a translation through a line parallel to that line of reflection (Park et al., 2008). A visual representation of each of these atomic geometrical symmetries is depicted in *Figure 1*.

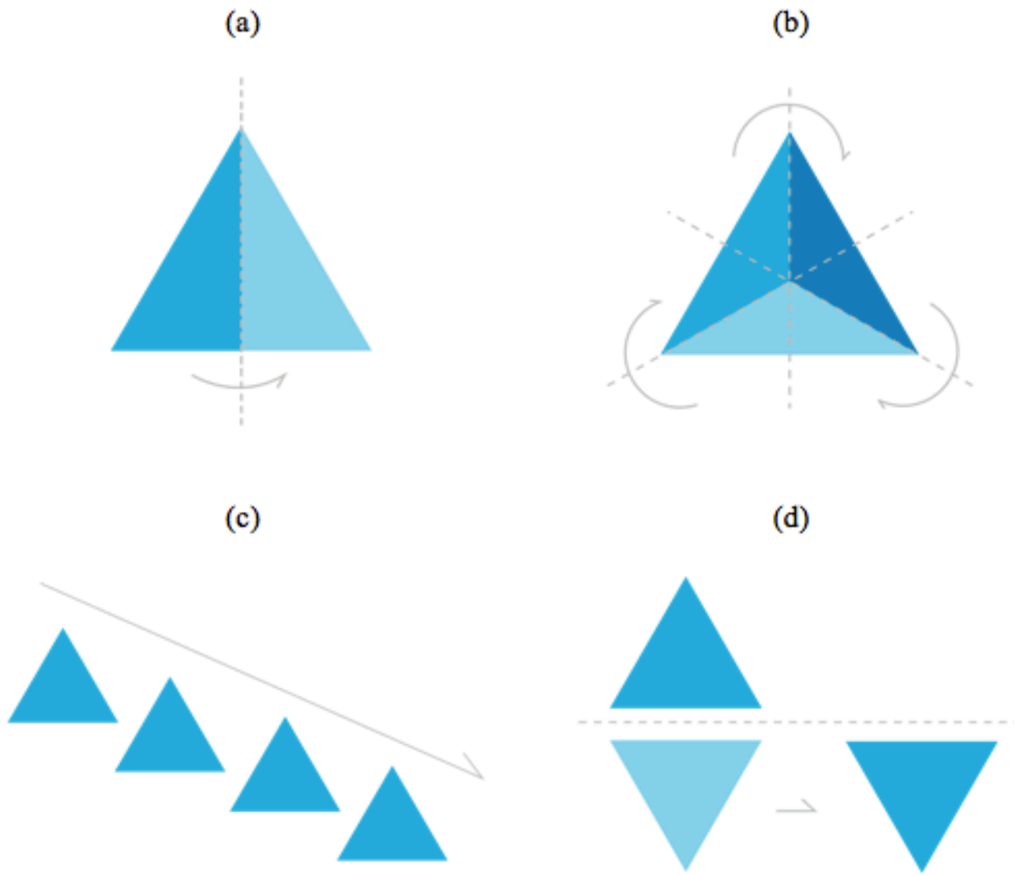

Figure 1. The four types of atomic geometrical symmetries, derived from the four Euclidean plane isometries. (a) Reflectional symmetry. (b) Rotational symmetry. (c) Translational symmetry. (d) Glide reflectional symmetry.

A single seed image, termed a *fundamental domain* (in Figure 1c and d above, it is a single equilateral triangle), can be subjected to any combination of the four isometries and then translated in two linearly independent dimensions to generate a regular two-dimensional pattern, or wallpaper. Examples of wallpapers generated from the same fundamental domain and subjected to each of the four isometries individually are depicted in *Figure 2*. The smallest area of the regular pattern that demonstrates all isometries of the pattern is termed the *unit*. Through different combinations of the four isometries, different orders of rotation (if there is rotational symmetry), and different directions of translation, distinct classes of these patterns can be created, called *wallpaper groups* (Schattschneider, 1978). Due to mathematical restrictions on the possible orders of rotation within a regular pattern, every repeating pattern in a two-dimensional plane can be classified into one of just 17 wallpaper groups. Does human perception reflect this deep mathematical regularity in some way?

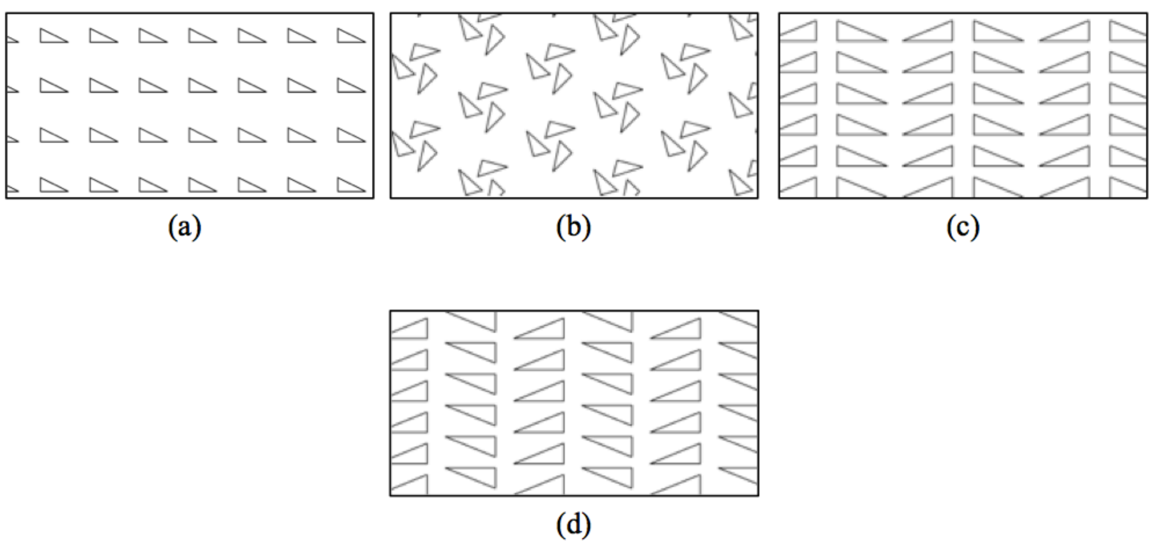

Figure 2. Sample wallpapers generated from the same triangle fundamental domain and subjected to only one of the four isometries. (a) Translation. (b) Rotation. (c) Reflection. (d) Glide reflection.

Theoretical Basis for Research

Clarke et al (2011) investigated the influence of symmetries on the perception of two-dimensional patterns. Specifically, the study measured the perceived similarity of exemplars of an individual wallpaper group to both 1) other exemplars of the same wallpaper group and, 2) exemplars of other wallpaper groups. The researchers generated 5 exemplars of each of the 17 wallpaper groups (for a total of 85 exemplars) by creating a functional domain from random-dot white noise and applying the appropriate isometries to make a regular pattern. The participants were presented with all 85 exemplars laid out randomly on a table, and instructed create subgroups by sorting them into as many piles as they desired using whatever criteria they saw appropriate.

Overall, the exemplars of the same wallpaper group were grouped together more frequently than expected by chance, indicating significant sensitivity to the wallpaper group classifications. However, substantial variability in the degree of self-similarity between wallpaper groups (as measured by the frequency that exemplars of a particular wallpaper group were placed in the same subset) indicated that the participants were taking other visual properties into account when classifying the images. Specifically, the particular fundamental domain used in creating each tiled pattern may have influenced the ability of the participants to detect the various symmetry patterns present in the stimuli.

The dot distribution within each seed fundamental domain could have influenced symmetry detection through differences in spatial frequency content. Spatial frequency is defined as the pattern of visual stimulus changes across space; thus, more detailed areas have a higher spatial frequency. In this manner, clusters—areas with higher dot density—could create regions of higher spatial frequency relative to the surrounding area. Julesz (1971) asserted a difference in the symmetry processing for patterns of differing spatial frequencies. Specifically, perception of symmetry in patterns with high spatial frequencies is relies more on point-by-point comparisons, whereas symmetric relations are extracted more globally in patterns with low spatial frequencies.

Moreover, the degree of non-uniformity in the pattern of dot distribution could affect the “goodness,” or overall perceptual salience, of individual exemplars. Nucci & Wagemans (2007) explored the impact of various local and global factors on the “goodness” of mirror symmetrical patterns. A sub-experiment varied the distance between dots and their symmetry axis and asked participants to classify the patterns as regular or random. The results found a positive correlation between the perceived goodness of a pattern and the proximity between the dots and their symmetry axis. Thus, the difference in perceived goodness of different exemplars could have provided an additional method of classification in the Clarke et al. (2011) study.

Variance in the dot number of the seed fundamental domains could have influenced symmetry detection, as well. Wenderoth (1996) investigated the impact of various dot pattern parameters on the perceived salience of bilateral symmetry. In one experiment, participants were presented with random-dot white noise patterns with varied symmetry axis orientations and dot numbers, and asked to classify the patterns as “symmetrical” or “random.” The results indicated that increasing the dot numbers magnified the disparity in salience between vertical and all other symmetries. This occurred because increasing the dot number did not have an effect on detecting vertical symmetries, but significantly detracted from the detection at other axis orientations.

Finally, variance in the dot density could impact symmetry detection. In another experiment, Wenderoth (1996) varied the dot density (i.e. the area that a set number of dots occupied) instead of the dot number, with the task classification remaining the same for the participants. This revealed an increased difficulty in detecting symmetry with higher dot densities. This effect could have emerged as another effect of the aforementioned variance in spatial frequencies. However, an alternative explanation exists involving luminance and contrast sensitivity. Zhang & Gerbino (1999) found that symmetry detection is impacted by differences in pattern luminance/contrast. Thus, differing amounts of white space due to dot density variance could impart this effect.

Thus, in the current study, we sought to understand how local elements influence the perception of global themes, with a particular emphasis on symmetry detection. In order to best control for symmetry and focus on disparities generated through variances in seed fundamental domains, we used five wallpaper groups rated highly self-similar in Clarke et al. (2011): P1, P3M1, P31M, P6, and P6M. Examples of these five wallpaper groups, with the same fundamental domain, are depicted in *Figure 3* to illustrate the symmetries present in and the global theme of each. Patterns were generated from random dots, but smoothed to reduce artifacts related to dot number and density. Patterns were also roughly equated for spatial frequency content. In addition, participants were interviewed after each task to informally assess their classification methodology.

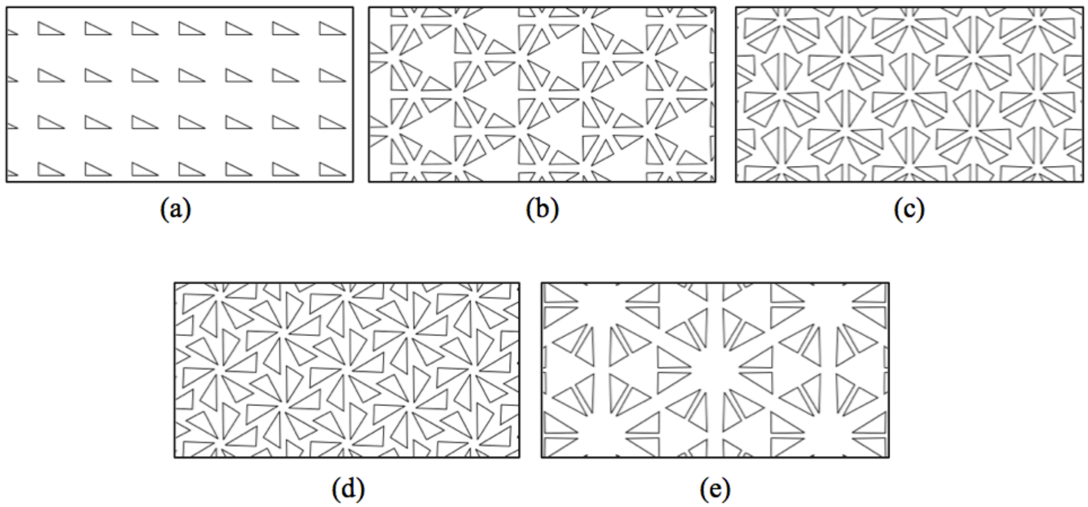

Figure 3. Examples of the five wallpaper groups used in this study, each with the same triangular fundamental domain. (a) P1. (b) P3M1. (c) P31M. (d) P6. (e) P6M.

Method

Participants

11 participants (8 male, 3 female), ranging in age between 19 and 23, were recruited as volunteers. All participants were naïve to the purpose of the study prior to the tasks, and lacked previous exposure to the topics inherent to the study.

Stimuli

Five wallpaper groups (P1, P3M1, P31M, P6, P6M) rated to be high in self-similarity, as determined by Clark et al (2011), were selected. 20 exemplars of each of these five wallpaper groups were created by tiling fundamental domains generated from random-dot white noise, resulting in a total of 100 distinct stimuli. These white noise fundamental domains had an area of ~4096 pixels, and were either square, rectangular, or triangular, depending on the symmetry group they represented. The advantages conferred by using white noise include the ability to generate numerous exemplars of the same wallpaper group and the absence of pattern discontinuities after tiling. These images were printed onto white cardstock and cut into squares, allowing participants to manipulate the orientation of the images during the sorting tasks. All stimuli are depicted (in reduced size) in Appendix A, organized by wallpaper group.

Procedure

Participants were presented with the 20 exemplars of a single wallpaper group (i.e. P1, P3M1, P31M, P6, P6M) and instructed to sort them into subsets by placing them into piles. Participants were advised to sort the exemplars into as many piles as they deemed necessary based on whatever criteria they desired. There were no time constraints placed on this sorting task, and the participants were allowed to move exemplars between piles until they were satisfied with their classification. This method was then repeated for the remaining four wallpaper groups for each participant, with group presentation order randomized between participants. These tasks were carried out on a large table with sufficient space to randomly lay out all twenty exemplars of each set, illuminated by normal overhead room lighting.

Upon completion of each sorting task, participants were asked to verbalize which features they used to sort the exemplars. After completion of all five sorting tasks, participants were asked which if they had a distinct method for sorting the images, and if any wallpaper group was particular easy or difficult to sort.

Generating the Jaccard Index

The data was prepared for analysis by creating one binary variable for each subset created by each participant within a sorting task. Then, each exemplar was assigned a value of one (1) if it was included in a subset, or a value zero (0) if it was not. Next, the similarity of each pair of exemplars within a sorting task was calculated using the Jaccard index, a distance similarity measure for binary data. This index is calculated by the equation $J = \frac{x}{x + y + z}$, with *x* representing the number of subsets that contained both exemplars, and *y* and *z* the number of subsets that contain only one exemplar of the pair (Capra, 2005). Thus, the Jaccard index is the ratio of the number of subsets containing both exemplars of a pair to the number of subsets containing at least one of the exemplars of a pair, thereby excluding subsets with joint absences.

Results

Pairs with the Highest Jaccard Scores

The Jaccard index was calculated for all pairs of the 20 exemplars within each of the five wallpaper groups, generating (20x19) 190 unique values for each wallpaper group. These values are depicted in a similarity matrix for each of the five wallpaper groups in Appendix B. After calculation of the distribution of values for each group, the Jaccard index for the pairs within the top 5% of the empirical distribution were selected as a representation of the most similar pairs; these are highlighted in blue within each similarity matrix.

Most- and Least- Representative Wallpaper Groups

The mean of all the Jaccard indices for each of the exemplars was calculated as a measure of the degree each exemplar fundamentally represented its respective wallpaper group. These values are depicted below each similarity matrix, with the highest and lowest values of each wallpaper group highlighted in green and red, respectively. The exemplars with the highest and lowest Jaccard index for each of the five wallpaper groups are depicted in Appendix C.

Variation of Jaccard Index between Wallpaper Groups

Assessment by boxplot, depicted in *Figure 4*, and a Shapiro-Wilk test (p <.001) revealed the presence of numerous outliers and severe non-normality in the data, violating a fundamental assumption required to perform an analysis of variance (ANOVA).

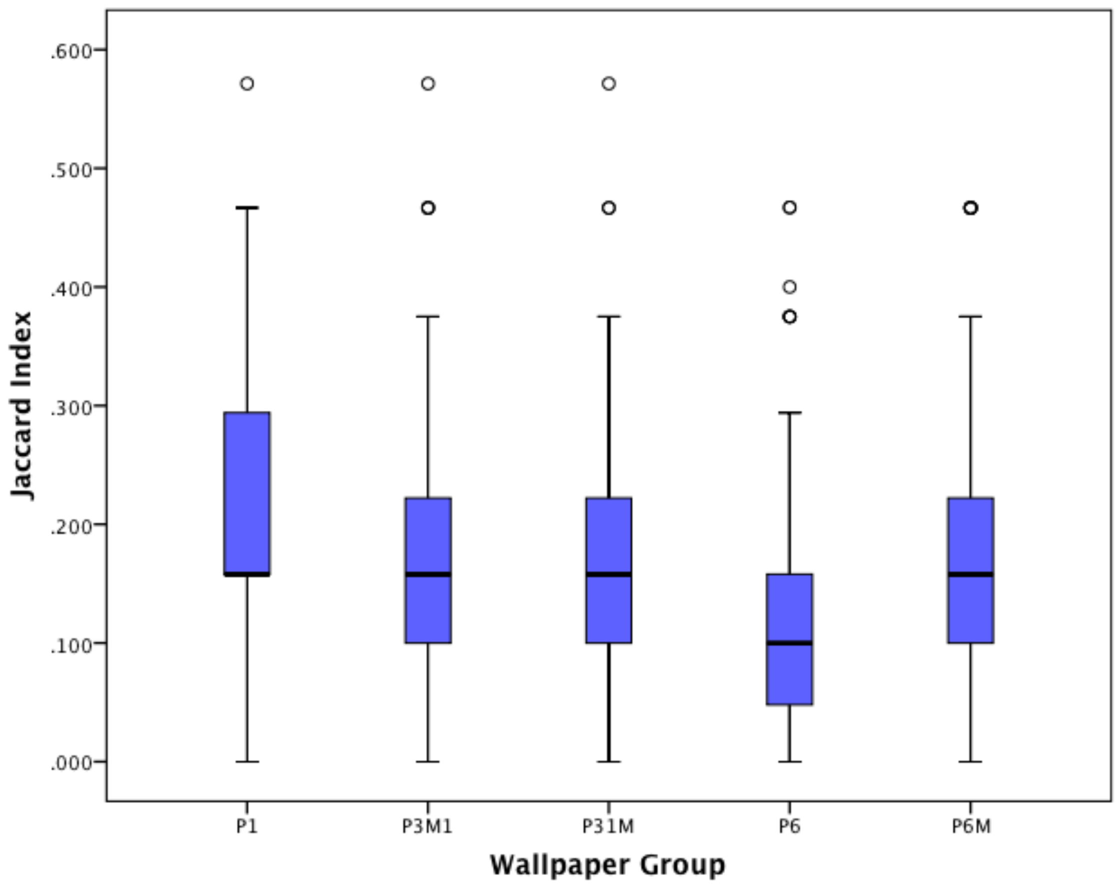

Figure 4. Boxplots of Jaccard index for each wallpaper group.

Thus, a Kruskal-Wallis test—the nonparametric equivalent of an ANOVA—was run to determine if there were differences in the Jaccard index between wallpaper groups. Pairwise comparisons were performed using Dunn's (1964) procedure with a Bonferroni correction for multiple comparisons. The Jaccard index was statistically significantly different between the different wallpaper groups, $\chi^2(4) = 61.648$, $p < .001$. Post-hoc analysis revealed statistically significant differences in the Jaccard index between the P1 (*Mdn* = .158) and P3M1 (*Mdn* = .158) (p <.001), P1 and P31M (*Mdn* = .158) (p <.001), P1 and P6 (*Mdn* = .100) (p <.001), P1 and P6M (*Mdn* = .158) (p <.05), and P6 and P6M (p <.001) wallpaper groups. Since median values were the same for each of the wallpaper groups aside from P6—which can occasionally occur with the Kruskal-Wallis test, as it is fundamentally a comparison of distributions, not medians—a different method was necessary for determining the relative differences between the groups. A histogram showing the distribution of Jaccard indices for each of the wallpaper groups, depicted in *Figure 5*, was used for this purpose (note: the boxplot cannot be used for this because it is fundamentally nonparametric). It is apparent that the distribution within P1 has significantly more Jaccard index values in the .200 to .300 range than the distributions of every other wallpaper group. Moreover, it appears that P6M has significantly more Jaccard index values in the same .200 to .300 range than P6. Both of these conclusions are validated by the results of the Kruskal-Wallis test.

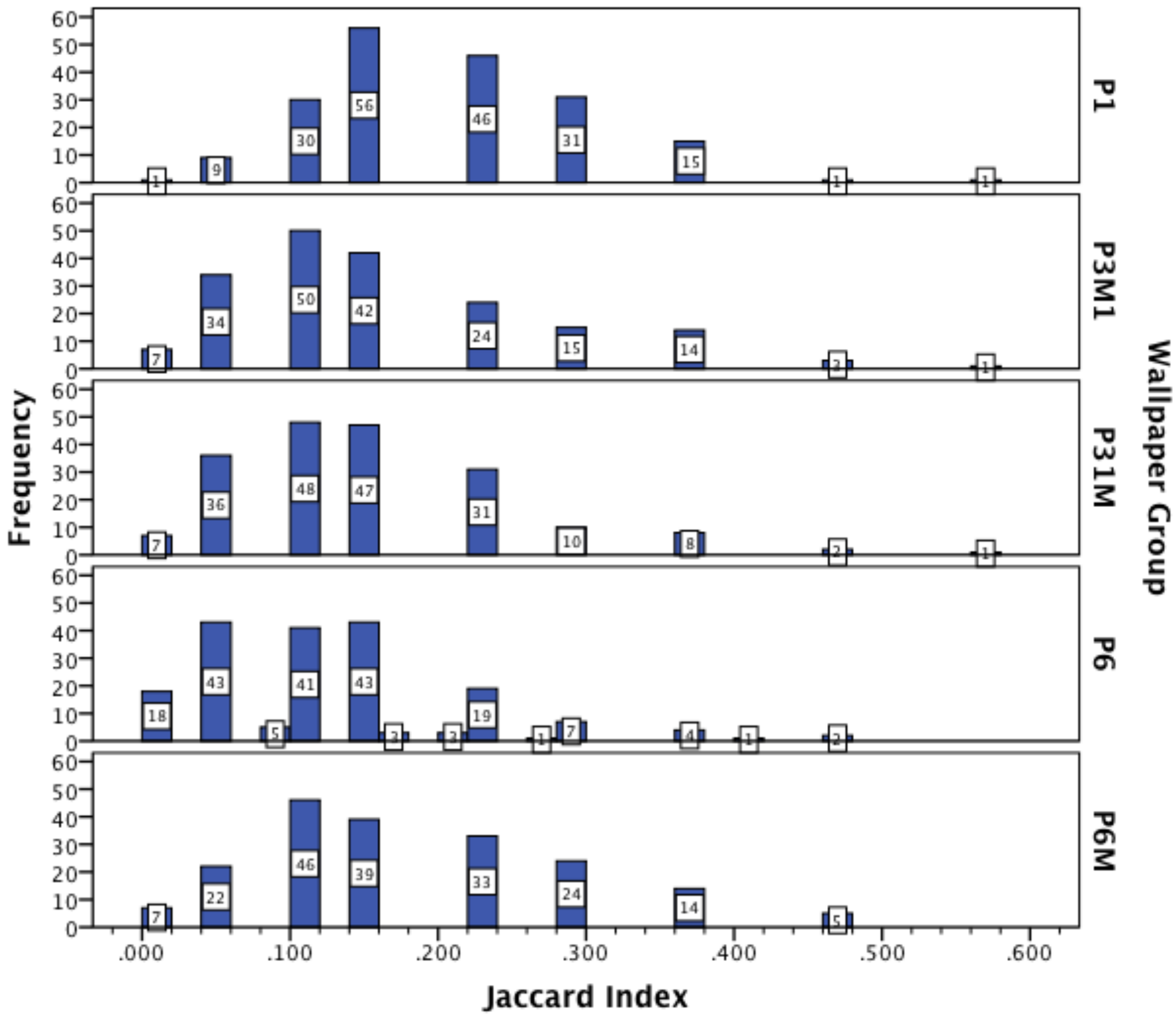

Figure 5. Histogram of Jaccard indices for each wallpaper group.

Variation of Subset Count between Wallpaper Groups

A repeated measures ANOVA was conducted to determine whether there were statistically significant differences in the number of subsets generated in the sorting task within each participant for each wallpaper group. Assessment of the boxplot, depicted in *Figure 6*, revealed no outliers, and the Shapiro-Wilk test ($p > .05$) revealed that the data were distributed normally. The assumption of sphericity was violated, as assessed by

Mauchly's Test of Sphericity, $\chi2(2) = 24.564$, $p = .004$. Therefore, a Greenhouse-Geisser correction was applied ($\varepsilon = 0.627$). The exercise intervention did not elicit statistically significant differences in subgroup number between wallpaper groups, $F(2.507, 25.073) = 2.468$, $p = .094$, with number of subgroups decreasing in order between P6 ($M = 5.545$, $SD = .755$), P31M ($M = 4.818$, $SD = .724$), P6M ($M = 4.636$, $SD = .730$), P31M ($M = 4.545$, $SD = .769$), and P1 ($M = 3.909$, $SD = .579$).

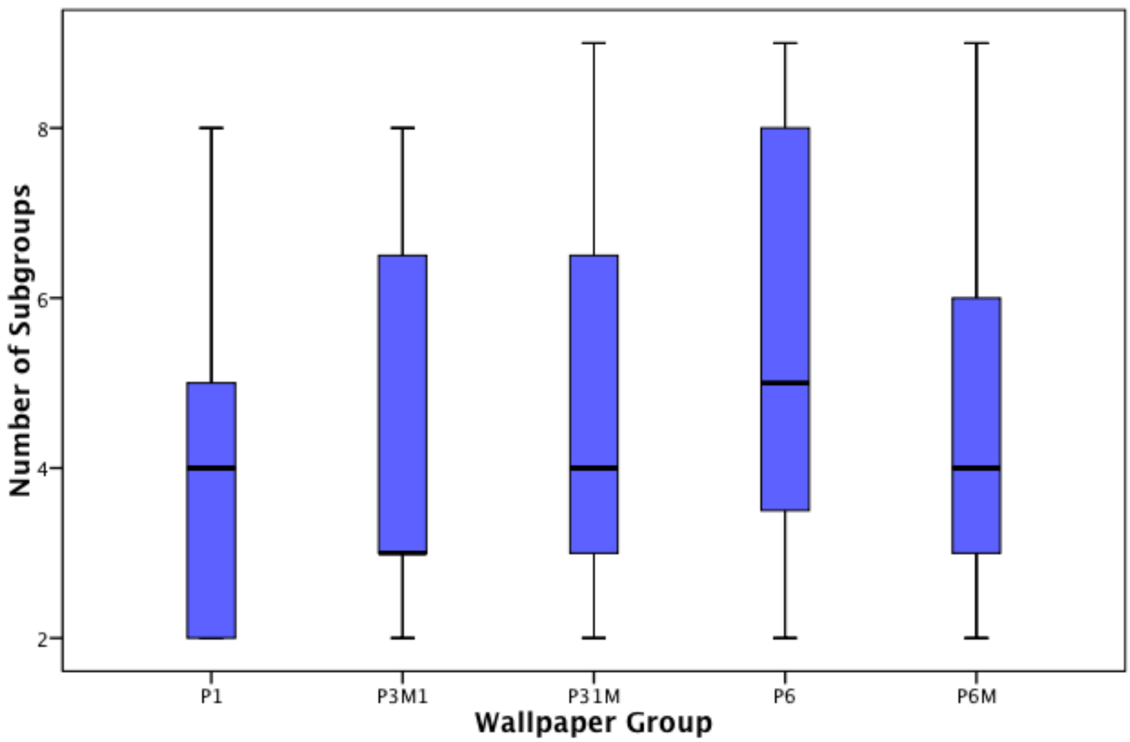

Figure 6. Boxplots of number of subgroups for each wallpaper group.

Discussion

The aim of this study was to explore the factors that influence sorting within an individual wallpaper group, and thereby possibly conclude why certain wallpaper groups are appear more self-similar than others. Our results show that the sorting of P1 resulted in sorted categories with a significantly higher Jaccard index distribution than all other wallpaper groups studied, indicating that participants sorted the P1 exemplars into similar sets (i.e. sets containing the same exemplars) significantly more often than in the other groups. The results of the repeated measures ANOVA indicates that this is not simply a byproduct of participants dividing the P1 exemplars into fewer subsets, thereby suggesting that there is less variation between participants in the factors used to sort the P1 group. Since Clark et al. (2011) demonstrated no significant link between the number of symmetries in a wallpaper group and its degree of self similarity, this lack of variation cannot be due to the inclusion of only one form of symmetry in P1. Thus, subjecting a seed fundamental domain to only translation symmetry must create a lower number of salient lower-order features compared to the rotations, reflections, and glide reflections. Indeed, all participants reported P1 as the most difficult group to sort due to lack of readily apparent features distinguishing the stimuli.

P6M was also found to have a significantly higher Jaccard index distribution than P6. Since the primary mathematical difference between P6M and P6 is the presence of reflectional symmetry in the former, this suggests reflectional symmetry could play a significant role in increasing self-similarity by providing a more salient grouping feature. This finding is supported by several studies that indicate reflectional symmetry is more readily detected and processed than the other forms of symmetry in humans (Swaddle, 1999).

Clark et al. (2011) observed that a similar global geometric structure emerges in all exemplars of each wallpaper group, regardless of the seed random dot fundamental domain used. These include striations, grid patterns, and large geometric forms with characteristic circular, triangular, or elliptical shapes. They further argued that the perceptual classification of wallpaper groups does not occur directly through the recognition of symmetries, but instead through the aforementioned characteristic global geometric structure. Thus, an exemplar with a high mean Jaccard index most likely has features that enhance the salience of that characteristic global geometric structure, thereby making it more perceptually similar to other exemplars of that group. The comparison of the exemplars with the highest and lowest mean Jaccard indices within a particular wallpaper group can elicit those features.

For P1 (as depicted in Figure C-1) the exemplar with the highest mean Jaccard index has more prominent straight lines running through the pattern, due to contrast differences. Indeed, some participants reported sorting the P1 exemplars by the appearance of these lines. This suggests that contrast can affect the salience of the global geometric structure—in this case, striations—especially in patterns with limited amounts of symmetry.

For P3M1 (as depicted in Figure C-2), the presence of the three-pronged black structure within each unit appears more salient than the large triangular geometric form in the exemplar with the lowest mean Jaccard index. Thus, a high contrast secondary structure within a unit can make it difficult to detect the global geometric structure.

For P31M (as depicted in Figure C-3), the exemplar with the highest mean Jaccard index prominently displays the 3rd-order rotational symmetry characteristic of the wallpaper group, whereas a lack of perceivable edges around the units in the other exemplar makes it harder to distinguish this feature. This suggests the importance of being able to discriminate the edges of a unit in recognizing the global geometric structure. This concept is further illustrated in comparing the exemplars within P6M (see Figure C-5).

For P6 (as depicted in Figure C-4), while the exemplar with the lowest mean Jaccard index clearly displays the edges of the unit, it does so at the sacrifice of prominently displaying the 6th-order rotational symmetry characteristic of the group, which the other exemplar does. This suggests the prominent role contrast plays in the determining the salience of distinct features within the pattern, and consequently the recognition of the global geometric structure.

The sorting task was not completed with any time restrictions, limiting the study’s generalizability in context of literature measuring the symmetry reaction times. Thus, these results cannot be fully used to evaluate models of symmetry detection, as classification decisions were made with more deliberation than would be afforded by time-limited sorting. This is also further clouded by the participants’ freedom to move images between subsets until they were satisfied, as higher order cognition could confound the reactions of the symmetry detection processes of the visual system.

Future studies could impose a time-restriction, effectively minimizing the aforementioned limitations. Moreover, the task could be repeated with stimuli that deliberately alter the factors—contrast, prominence of unit outline, and presence of salient secondary structures—suggested to influence the salience of the global geometric structure inherent to each wallpaper group. The paradigm could also be restructured so that participants judge the similarity of only two exemplars at a time using a Likert-scale. Combined with a cluster analysis, this experimental design could further explore whether the human visual system perceptually organizes wallpaper groups in the hierarchical structure predicted by group theoretical mathematics (Schattschneider, 1978).

Based on the aforementioned uses of symmetry detection within the human visual system, and the abundance of visual symmetry in the real world, the potential benefits of being able to effectively artificially recreate this mechanism within computers is clear. Potential applications of computational symmetry include facial recognition, 3D-reconstruction, and image resolution-enhancement (Park et al., 2008). However, even after over 30 years of research, the best computer algorithm has a mean sensitivity of only 42% for bilateral reflection symmetry, and 32% for rotational symmetry, with a 43% and 13% false positive rate, respectively (Park et al., 2008). It is possible that the human mechanism of symmetry perception is particularly efficient and effective, and thus gaining a better understanding of these processes could, in turn, inform computer vision as well.

Appendix A: Stimuli

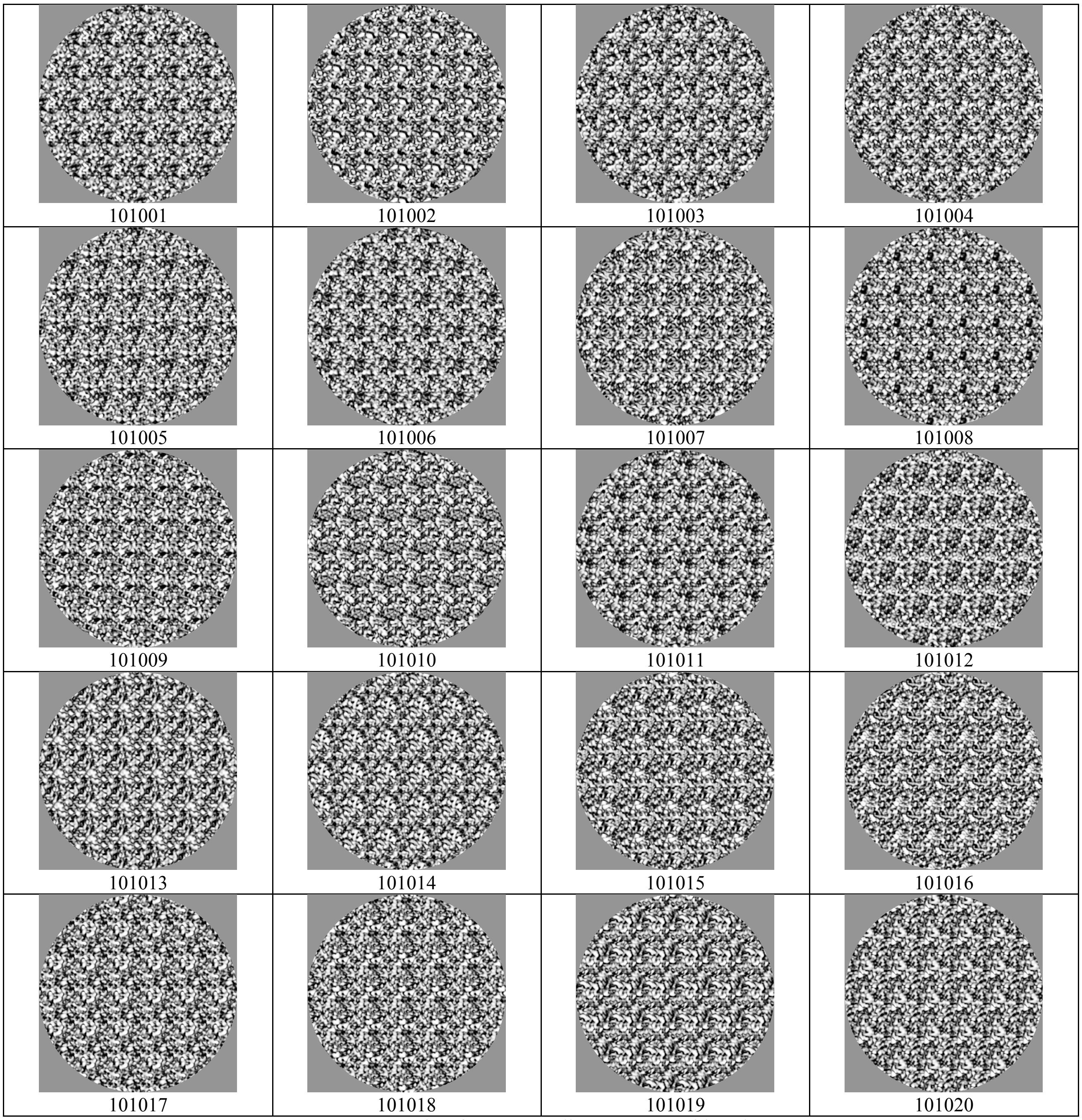

Figure A-1. Exemplars for P3M1 wallpaper group, with code names.

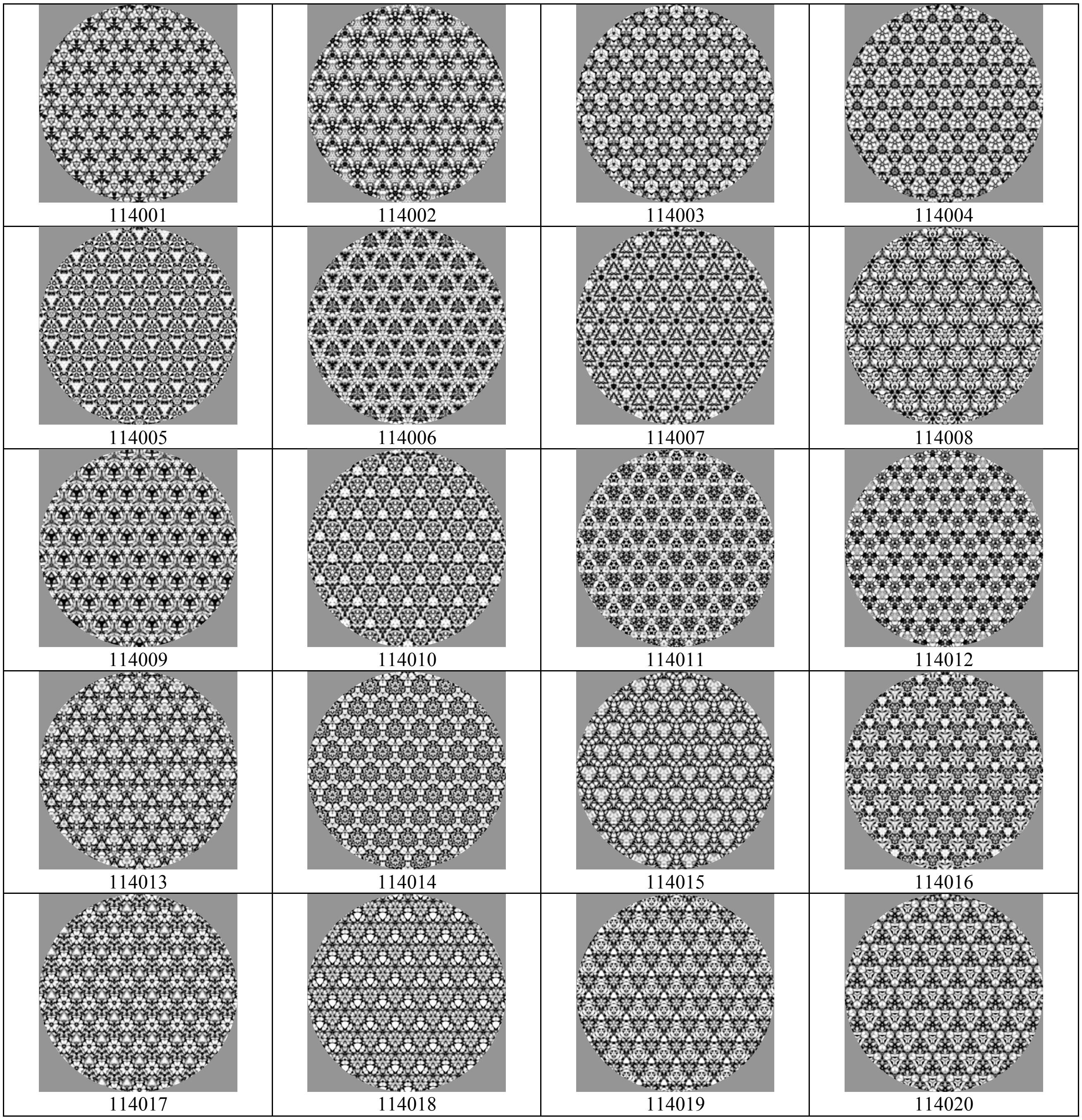

Figure A-2. Exemplars for P3M1 wallpaper group, with code names.

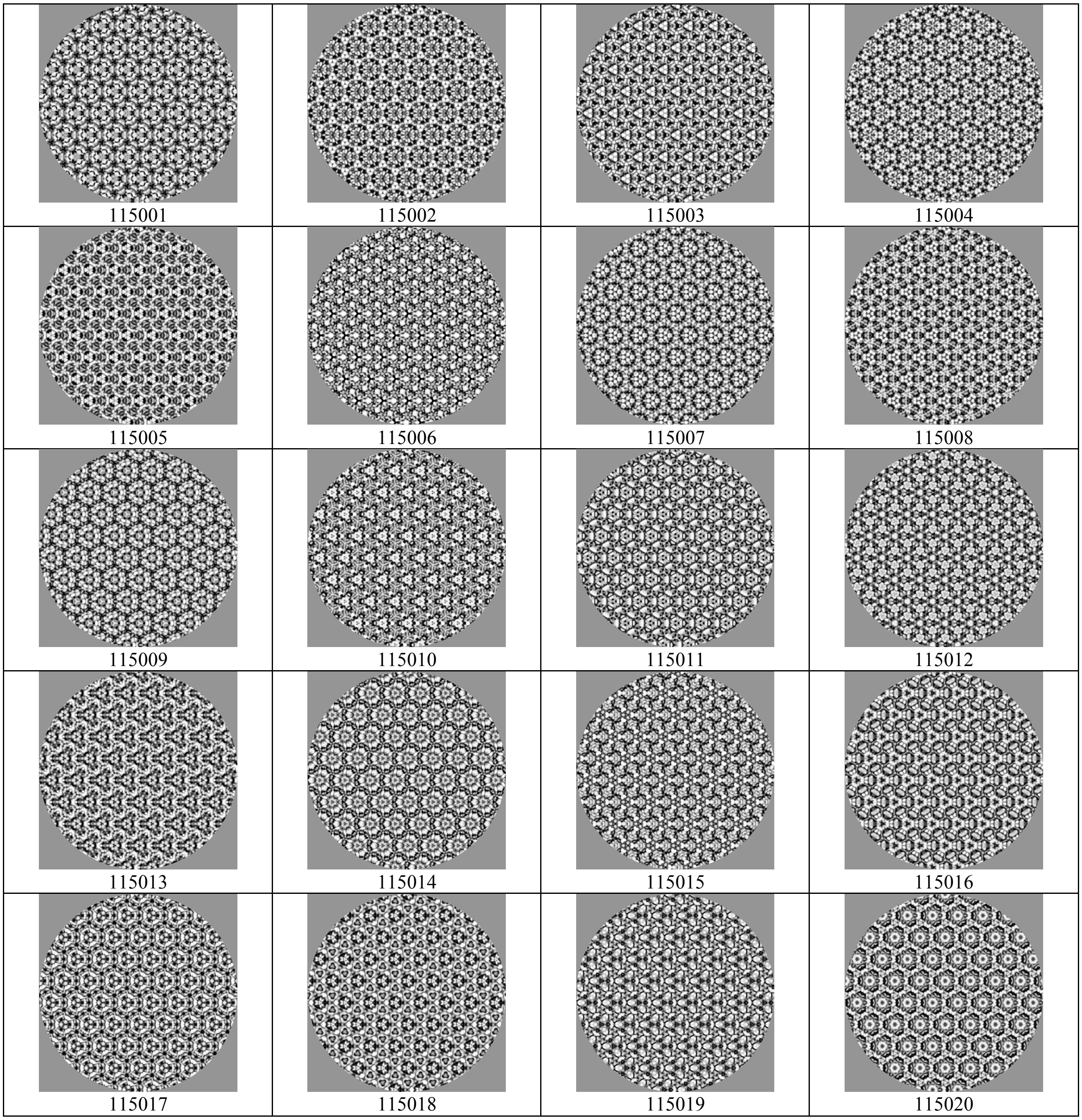

Figure A-3. Exemplars for P31M wallpaper group, with code names.

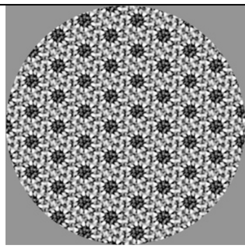 116001	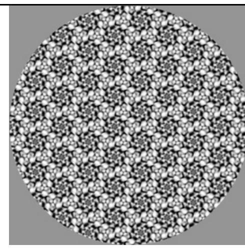 116002	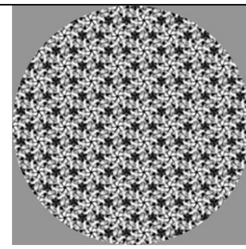 116003	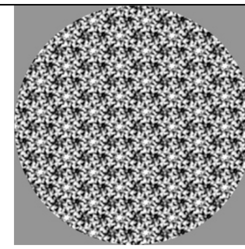 116004
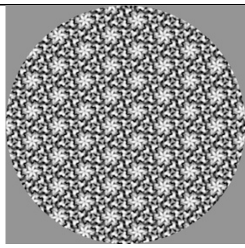 116005	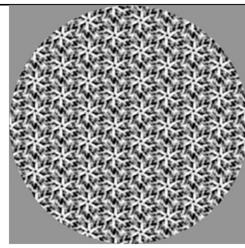 116006	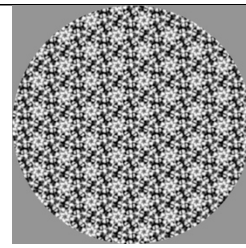 116007	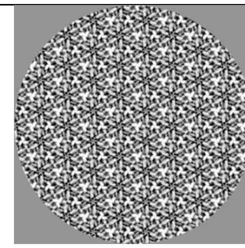 116008
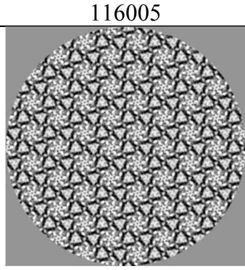 116009	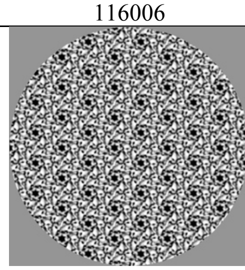 116010	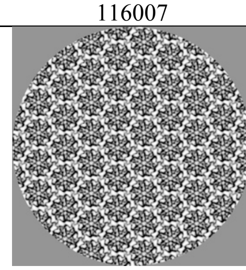 116011	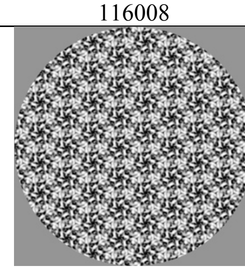 116012
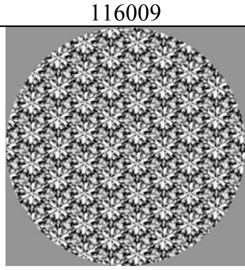 116013	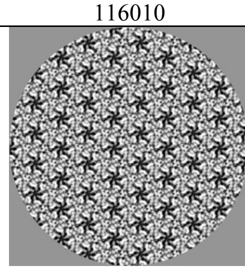 116014	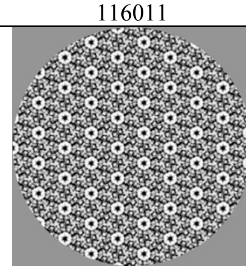 116015	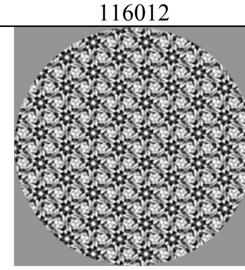 116016
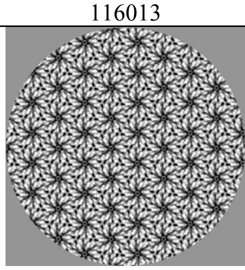 116017	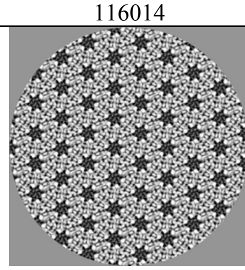 116018	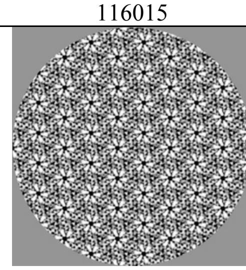 116019	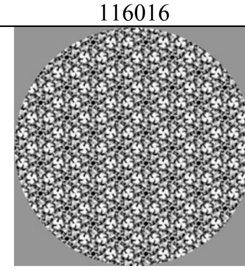 116020

Figure A-4. Exemplars for P6 wallpaper group, with code names.

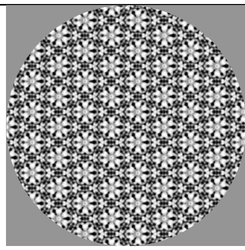 117001	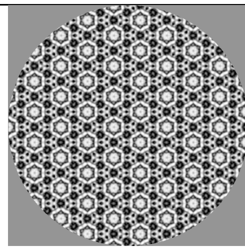 117002	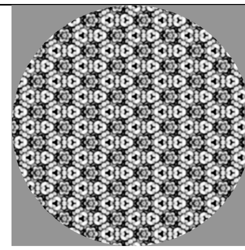 117003	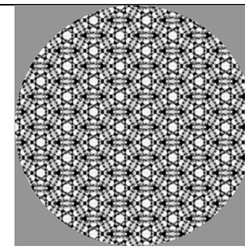 117004
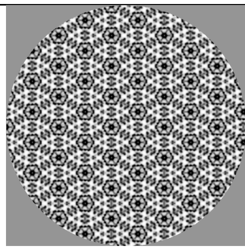 117005	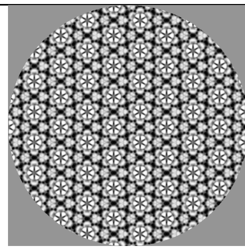 117006	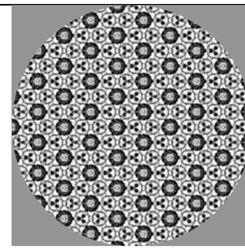 117007	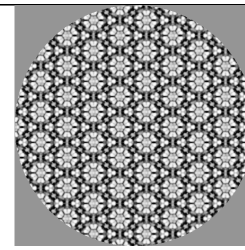 117008
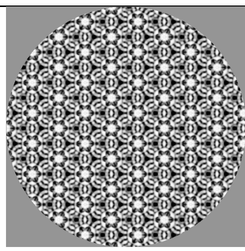 117009	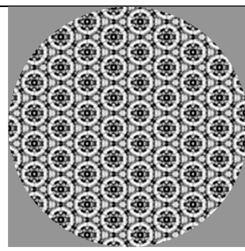 117010	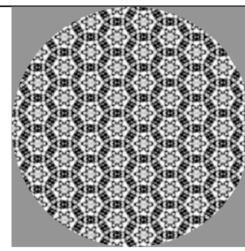 117011	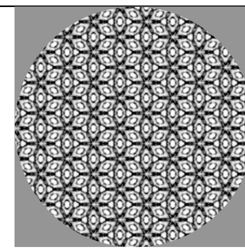 117012
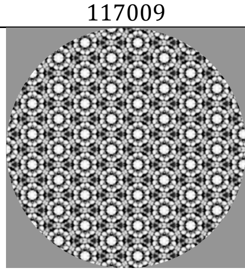 117013	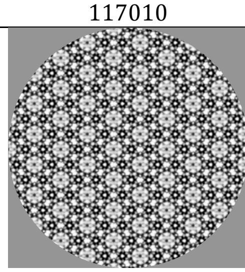 117014	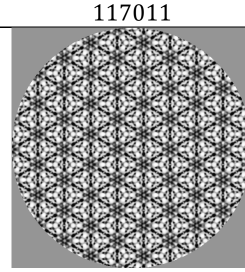 117015	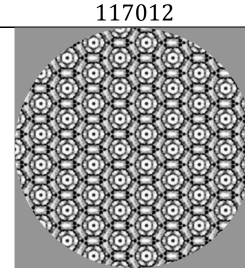 117016
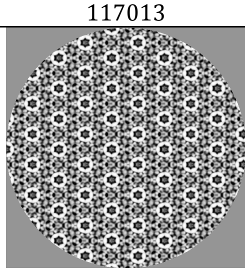 117017	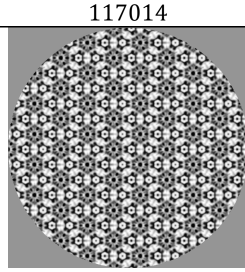 117018	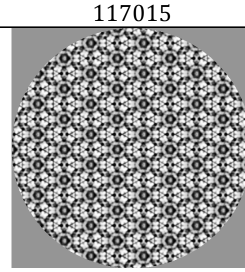 117019	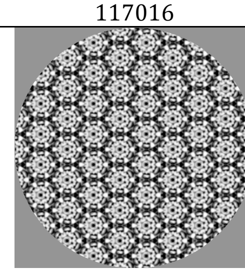 117020

Figure A-5. Exemplars for P6M wallpaper group, with code names.

Appendix B: Similarity Matrices

	Jaccard Measure																			
	101001	101002	101003	101004	101005	101006	101007	101008	101009	101010	101011	101012	101013	101014	101015	101016	101017	101018	101019	101020
101001		.375	.100	.100	.222	.100	.100	.222	.375	.294	.294	.158	.222	.100	.294	.222	.375	.158	.158	.158
101002	.375		.100	.100	.222	.222	.158	.158	.294	.222	.222	.048	.158	.158	.158	.158	.048	.158	.222	.100
101003	.100	.100		.158	.222	.158	.294	.158	.100	.222	.294	.375	.222	0.294	.375	.222	.375	.158	.294	.294
101004	.100	.100	.158		.158	.222	.100	.158	.100	.375	.158	.222	.158	.158	.222	.158	.222	.158	.048	.158
101005	.222	.222	.222	.158		.222	.294	.100	.294	.100	.222	.222	.375	.294	.294	.222	.100	.294	.100	.100
101006	.100	.222	.158	.222	.222		.222	.048	.048	.158	.158	.158	.222	.158	.294	.222	.158	0.158	.100	.100
101007	.100	.158	.294	.100	.294	.222		.100	0.158	.158	.100	.375	.158	.375	.294	.294	.222	.100	.571	.294
101008	.222	.158	.158	.158	.100	.048	.100		.467	.222	.158	.100	.158	.158	.048	.222	.222	.158	.158	.158
101009	.375	.294	.100	.100	.294	.048	0.158	.467		.222	.222	.158	.222	.100	.158	.100	.158	.294	.158	.100
101010	.294	.222	.222	.375	.100	.158	.158	.222	.222		.222	.158	.100	.158	.294	.294	.222	.048	.222	.294
101011	.294	.222	.294	.158	.222	.158	.100	.158	.222	.222		.100	.294	.222	.158	.048	.222	.222	.158	.158
101012	.158	.048	.375	.222	.222	.158	.375	.100	.158	.158	.100		.222	0.294	.375	.158	.294	.048	.375	0.294
101013	.222	.158	.222	.158	.375	.222	.158	.158	.222	.100	.294	.222		.158	.222	.222	.158	.294	.100	.222
101014	.100	.158	0.294	.158	.294	.158	.375	.158	.100	.158	.222	0.294	.158		0.158	.222	.222	.158	.222	.375
101015	.294	.158	.375	.222	.294	.294	.294	.048	.158	.294	.158	.375	.222	0.158		.222	.294	.158	.294	.222
101016	.222	.158	.222	.158	.222	.222	.294	.222	.100	.294	.048	.158	.222	.222	.222		.294	.100	.158	.294
101017	.375	.048	.375	.222	.100	.158	.222	.222	.158	.222	.222	.294	.158	.222	.294	.294		0.158	.158	.375
101018	.158	.158	.158	.158	.294	0.158	.100	.158	.294	.048	.222	.048	.294	.158	.158	.100	0.158		.000	.100
101019	.158	.222	.294	.048	.100	.100	.571	.158	.158	.222	.158	.375	.100	.222	.294	.158	.158	.000		.375
101020	.158	.100	.294	.158	.100	.100	.294	.158	.100	.294	.158	0.294	.222	.375	.222	.294	.375	.100	.375	
Mean	0.212	0.1727	0.2324	0.1649	0.2136	0.1646	0.2299	0.1669	0.1962	0.2098	0.1912	0.2176	0.2047	0.2097	0.2387	0.2018	0.2251	0.1537	0.2038	0.2196

Figure B-1. Similarity matrix for P1. Values highlighted in blue indicate top 5% of Jaccard indices. Values highlighted in green and red indicate highest and lowest Jaccard indices, respectively.

	Jaccard Measure																			
	114001	114002	114003	114004	114005	114006	114007	114008	114009	114010	114011	114012	114013	114014	114015	114016	114017	114018	114019	114020
114001		.048	.294	.100	.100	.158	.158	.158	.158	.100	.048	.158	.375	.158	.375	.294	.158	.158	.222	.100
114002	.048		.100	.222	.048	.222	.048	.222	.048	.100	.100	.375	.158	.158	.158	.158	.222	.158	.000	.158
114003	.294	.100		.222	.158	.100	.158	.158	.100	.375	.100	.158	.222	0.100	.048	.294	.467	.222	.100	.000
114004	.100	.222	.222		.222	.048	.158	.222	.048	.375	.158	.100	.158	.158	.100	.294	.158	.222	.100	.158
114005	.100	.048	.158	.222		.100	.375	.100	.222	.222	.158	.048	.048	.100	.100	.048	.158	.158	.100	.100
114006	.158	.222	.100	.048	.100		.158	.000	.294	.100	.294	.158	.048	.048	.222	.048	.100	0.048	.375	.294
114007	.158	.048	.158	.158	.375	.158		.048	0.375	.100	.100	.000	.048	.048	.222	.048	.100	.222	.222	.158
114008	.158	.222	.158	.222	.100	.000	.048		.000	.158	.158	.294	.467	.294	.158	.158	.222	.294	.048	.100
114009	.158	.048	.100	.048	.222	.294	0.375	.000		.100	.048	.048	.100	.100	.222	.048	.158	.048	.158	.100
114010	.100	.100	.375	.375	.222	.100	.100	.158	.100		.222	.294	.158	.048	.100	.222	.222	.158	.100	.158
114011	.048	.100	.100	.158	.158	.294	.100	.158	.048	.222		.158	.100	.158	.222	.100	.048	.158	.375	.375
114012	.158	.375	.158	.100	.048	.158	.000	.294	.048	.294	.158		.294	0.100	.100	.100	.375	.100	.048	0.100
114013	.375	.158	.222	.158	.048	.048	.048	.467	.100	.158	.100	.294		.294	.294	.294	.375	.100	.100	.100
114014	.158	.158	0.100	.158	.100	.048	.048	.294	.100	.048	.158	0.100	.294		0.100	.222	.100	.100	.048	.100
114015	.375	.158	.048	.100	.100	.222	.222	.158	.222	.100	.222	.100	.294	0.100		.048	.100	.000	.375	.467
114016	.294	.158	.294	.294	.048	.048	.048	.158	.048	.222	.100	.100	.294	.222	.048		.100	.375	.048	.048
114017	.158	.222	.467	.158	.158	.100	.100	.222	.158	.222	.048	.375	.375	.100	.100	.100		0.100	.048	.048
114018	.158	.158	.222	.222	.158	0.048	.222	.294	.048	.158	.158	.100	.100	.100	.000	.375	0.100		.048	.000
114019	.222	.000	.100	.100	.100	.375	.222	.048	.158	.100	.375	.048	.100	.048	.375	.048	.048	.048		.571
114020	.100	.158	.000	.158	.100	.294	.158	.100	.100	.158	.375	0.100	.100	.100	.467	.048	.048	.000	.571	
Mean	0.17468	0.1422	0.1777	0.1696	0.1349	0.1481	0.1444	0.1715	0.1249	0.1743	0.162	0.1583	0.1964	0.128	0.1795	0.155	0.1715	0.1404	0.1623	0.164949

Figure B-2. Similarity Matrix for P3M1. Values highlighted in blue indicate top 5% of Jaccard indices. Values highlighted in green and red indicate highest and lowest Jaccard indices, respectively.

	Jaccard Measure																			
	115001	115002	115003	115004	115005	115006	115007	115008	115009	115010	115011	115012	115013	115014	115015	115016	115017	115018	115019	115020
115001		.000	.158	.158	.100	.048	.048	.100	.375	.100	.158	.294	.158	.048	.158	.000	.158	.048	.222	.000
115002	.000		.048	.100	.100	.158	.571	.048	.158	.158	.048	.100	.048	.375	.100	.222	.375	.100	.100	.375
115003	.158	.048		.100	.294	.048	.100	.222	.158	.158	.048	.158	.100	0.048	.100	.100	.100	.100	.222	.048
115004	.158	.100	.100		.100	.222	.048	.222	.375	.048	.222	.048	.158	.158	.158	.158	.100	.294	.158	.158
115005	.100	.100	.294	.100		.100	.222	.100	.048	.048	.048	.294	.048	.000	.100	.100	.048	.294	.000	.048
115006	.048	.158	.048	.222	.100		.100	.222	.048	.158	.222	.158	.158	.158	.294	.375	.222	0.222	.222	.100
115007	.048	.571	.100	.048	.222	.100		.100	0.048	.158	.000	.158	.100	.222	.048	.158	.222	.048	.048	.375
115008	.100	.048	.222	.222	.100	.222	.100		.048	.100	.048	.222	.222	.100	.222	.158	.100	.158	.222	.048
115009	.375	.158	.158	.375	.048	.048	0.048	.048		.158	.158	.100	.100	.222	.100	.048	.100	.100	.222	.100
115010	.100	.158	.158	.048	.048	.158	.158	.100	.158		.100	.048	.294	.158	.222	.222	.158	.100	.158	.294
115011	.158	.048	.048	.222	.048	.222	.000	.048	.158	.100		.048	.158	.222	.222	.222	.100	.158	.158	.100
115012	.294	.100	.158	.048	.294	.158	.158	.222	.100	.048	.048		.100	0.000	.100	.048	.100	.158	.100	0.048
115013	.158	.048	.100	.158	.048	.158	.100	.222	.100	.294	.158	.100		.158	.158	.222	.100	.222	.158	.158
115014	.048	.375	0.048	.158	.000	.158	.222	.100	.222	.158	.222	0.000	.158		0.222	.222	.222	.100	.100	.467
115015	.158	.100	.100	.158	.100	.294	.048	.222	.100	.222	.222	.100	.158	0.222		.158	.100	.158	.467	.158
115016	.000	.222	.100	.158	.100	.375	.158	.158	.048	.222	.222	.048	.222	.222	.158		.294	.375	.158	.158
115017	.158	.375	.100	.100	.048	.222	.222	.100	.100	.158	.100	.100	.100	.222	.100	.294		0.048	.158	.294
115018	.048	.100	.100	.294	.294	0.222	.048	.158	.100	.100	.158	.158	.222	.100	.158	.375	0.048		.158	.048
115019	.222	.100	.222	.158	.000	.222	.048	.222	.222	.158	.158	.100	.158	.100	.467	.158	.158	.158		.100
115020	.000	.375	.048	.158	.048	.100	.375	.048	.100	.294	.100	0.048	.158	.467	.158	.158	.294	.048	.100	
Mean	0.1226	0.1675	0.1215	0.157	0.11002	0.1703	0.1459	0.1401	0.1402	0.1494	0.1284	0.12	0.1484	0.1685	0.1708	0.1788	0.1578	0.152	0.1648	0.1618

Figure B-3. Similarity matrix for P4M1. Values highlighted in blue indicate top 5% of Jaccard indices. Values highlighted in green and red indicate highest and lowest Jaccard indices, respectively.

	Jaccard Measure																			
	116001	116002	116003	116004	116005	116006	116007	116008	116009	116010	116011	116012	116013	116014	116015	116016	116017	116018	116019	116020
116001		.222	.048	.048	.211	.000	.048	.000	.000	.048	.100	.100	.048	.158	.235	.100	.222	.222	.158	.158
116002	.222		.158	.100	.150	.048	.048	.000	.100	.100	.375	.222	.100	.158	.105	.294	.158	.100	.158	.100
116003	.048	.158		.222	.095	.222	.158	.048	.100	.222	.100	.158	.158	0.294	.050	.158	.222	.048	.158	.100
116004	.048	.100	.222		.095	.048	.158	.000	.048	.294	.158	.294	.048	.100	.167	.158	.100	.100	.100	.100
116005	.211	.150	.095	.095		.095	.150	.095	.150	.045	.150	.150	.278	.045	.048	.045	.095	.000	.211	.211
116006	.000	.048	.222	.048	.095		.158	.222	.222	.100	.048	.048	.375	.158	.050	.158	.048	0.100	.375	.048
116007	.048	.048	.158	.158	.150	.158		.158	0.294	.100	.100	.158	.158	.000	.105	.222	.048	.048	.100	.048
116008	.000	.000	.048	.000	.095	.222	.158		.294	.048	.100	.000	.100	.048	.050	.048	.000	.048	.048	.375
116009	.000	.100	.100	.048	.150	.222	0.294	.294		.100	.158	.222	.158	.000	.105	.158	.000	.048	.048	.100
116010	.048	.100	.222	.294	.045	.100	.100	.048	.100		.048	.100	.158	.100	.400	.222	.100	.158	.048	.000
116011	.100	.375	.100	.158	.150	.048	.100	.100	.158	.048		.158	.000	.048	.105	.100	.100	.000	.048	.100
116012	.100	.222	.158	.294	.150	.048	.158	.000	.222	.100	.158		.100	0.222	.050	.222	.158	.100	.100	0.158
116013	.048	.100	.158	.048	.278	.375	.158	.100	.158	.158	.000	.100		.158	.050	.158	.158	.158	.467	.000
116014	.158	.158	0.294	.100	.045	.158	.000	.048	.000	.100	.048	0.222	.158		0.000	.158	.467	.222	.158	.158
116015	.235	.105	.050	.167	.048	.050	.105	.050	.105	.400	.105	.050	.050	0.000		.167	.000	.167	.050	.050
116016	.100	.294	.158	.158	.045	.158	.222	.048	.158	.222	.100	.222	.158	.158	.167		.158	.158	.100	.000
116017	.222	.158	.222	.100	.095	.048	.048	.000	.000	.100	.100	.158	.158	.467	.000	.158		0.294	.222	.100
116018	.222	.100	.048	.100	.000	0.100	.048	.048	.048	.158	.000	.100	.158	.222	.167	.158	0.294		.222	.048
116019	.158	.158	.158	.100	.211	.375	.100	.048	.048	.048	.048	.100	.467	.158	.050	.100	.222	.222		.048
116020	.158	.100	.100	.100	.211	.048	.048	.375	.100	.000	.100	0.158	.000	.158	.050	.000	.100	.048	.048	
Mean	0.1118	0.1419	0.1431	0.123	0.12208	0.1327	0.1188	0.0884	0.1213	0.1258	0.105	0.1432	0.1488	0.1395	0.1028	0.1465	0.1394	0.1179	0.1482	.100

Figure B-4. Similarity matrix for P6. Values highlighted in blue indicate top 5% of Jaccard indices. Values highlighted in green and red indicate highest and lowest Jaccard indices, respectively.

	Jaccard Measure																			
	117001	117002	117003	117004	117005	117006	117007	117008	117009	117010	117011	117012	117013	117014	117015	117016	117017	117018	117019	117020
117001		.158	.294	.158	.100	.222	.100	.048	.294	.100	.467	.222	.158	.100	.294	.100	.100	.100	.158	.222
117002	.158		.048	.158	.294	.294	.048	.467	.375	.375	.100	.048	.158	.222	.100	.158	.222	.048	.375	.375
117003	.294	.048		.100	.100	.100	.294	.048	.158	.048	.294	.100	.222	0.000	.375	.100	.100	.467	.100	.100
117004	.158	.158	.100		.222	.100	.100	.100	.222	.100	.294	.100	.158	.158	.100	.222	.100	.294	.100	.222
117005	.100	.294	.100	.222		.100	.222	.100	.100	.158	.158	.100	.158	.158	.158	.158	.294	.158	.222	.294
117006	.222	.294	.100	.100	.100		.100	.222	.222	.375	.222	.100	.294	.294	.158	.100	.375	0.000	.294	.158
117007	.100	.048	.294	.100	.222	.100		.100	0.000	.048	.100	.048	.222	.158	.222	.158	.222	.222	.100	.158
117008	.048	.467	.048	.100	.100	.222	.100		.222	.467	.048	.048	.222	.375	.100	.375	.100	.048	.294	.294
117009	.294	.375	.158	.222	.100	.222	0.000	.222		.222	.158	.048	.158	.222	.100	.222	.100	.158	.294	.222
117010	.100	.375	.048	.100	.158	.375	.048	.467	.222		.100	.048	.294	.375	.158	.294	.158	.048	.375	.375
117011	.467	.100	.294	.294	.158	.222	.100	.048	.158	.100		.222	.158	.048	.294	.048	.158	.100	.158	.100
117012	.222	.048	.100	.100	.100	.100	.048	.048	.048	.048	.222		.048	0.000	.375	.048	.048	.222	.222	0.000
117013	.158	.158	.222	.158	.158	.294	.222	.222	.158	.294	.158	.048		.222	.222	.467	.158	.100	.158	.294
117014	.100	.222	0.000	.158	.158	.294	.158	.375	.222	.375	.048	0.000	.222		0.000	.294	.158	.048	.222	.294
117015	.294	.100	.375	.100	.158	.158	.222	.100	.100	.158	.294	.375	.222	0.000		.100	.100	.375	.222	.158
117016	.100	.158	.100	.222	.158	.100	.158	.375	.222	.294	.048	.048	.467	.294	.100		.048	.158	.158	.294
117017	.100	.222	.100	.100	.294	.375	.222	.100	.100	.158	.158	.048	.158	.158	.100	.048		0.000	.158	.158
117018	.100	.048	.467	.294	.158	0.000	.222	.048	.158	.048	.100	.222	.100	.048	.375	.158	0.000		.158	.100
117019	.158	.375	.100	.100	.222	.294	.100	.294	.294	.375	.158	.222	.158	.222	.222	.158	.158	.158		.222
117020	.222	.375	.100	.222	.294	.158	.158	.294	.222	.375	.100	0.000	.294	.294	.158	.294	.158	.100	.222	
Mean	0.1787	0.2117	0.1604	0.1584	0.17128	0.1964	0.138	0.1935	0.1841	0.2166	0.1698	0.1076	0.2037	0.1762	0.1901	0.1843	0.1451	0.1475	0.21	0.2127

Figure B-5. Similarity matrix for P6M. Values highlighted in blue indicate top 5% of Jaccard indices. Values highlighted in green and red indicate highest and lowest Jaccard indices, respectively.

Appendix C: Exemplars with Highest and Lowest Mean Jaccard Indices

	P1 Exemplars	Mean Jaccard index
(a)	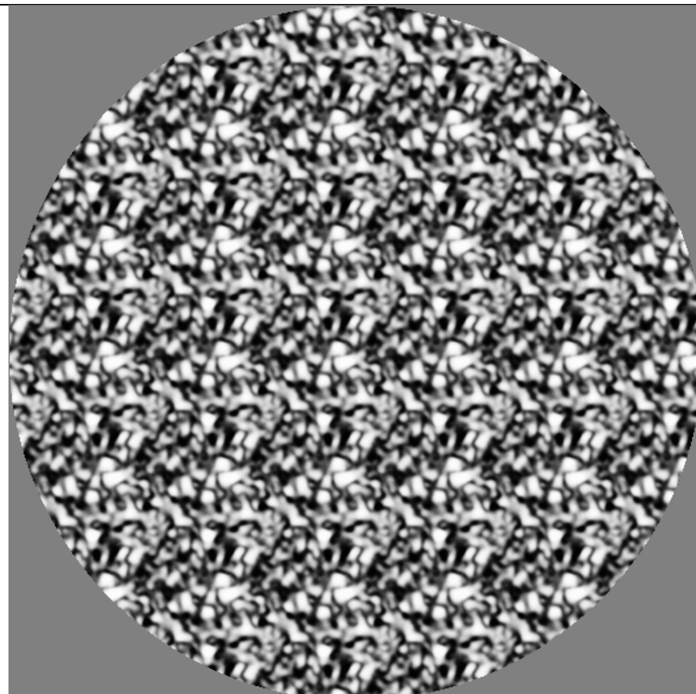	.2387
(b)	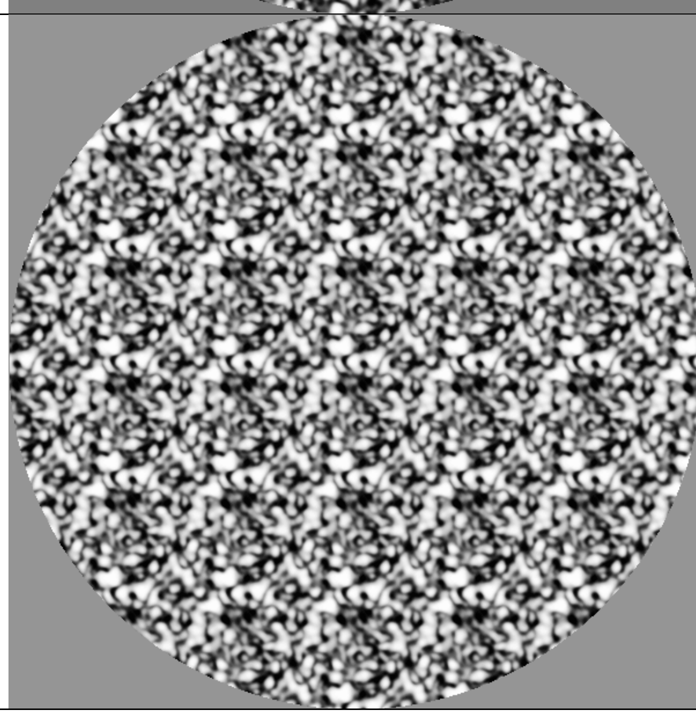	.1537

Figure C-1. P1. (a) Exemplar with highest mean Jaccard index. (b) Exemplar with lowest mean Jaccard index.

	P3M1 Exemplars	Mean Jaccard index
(a)	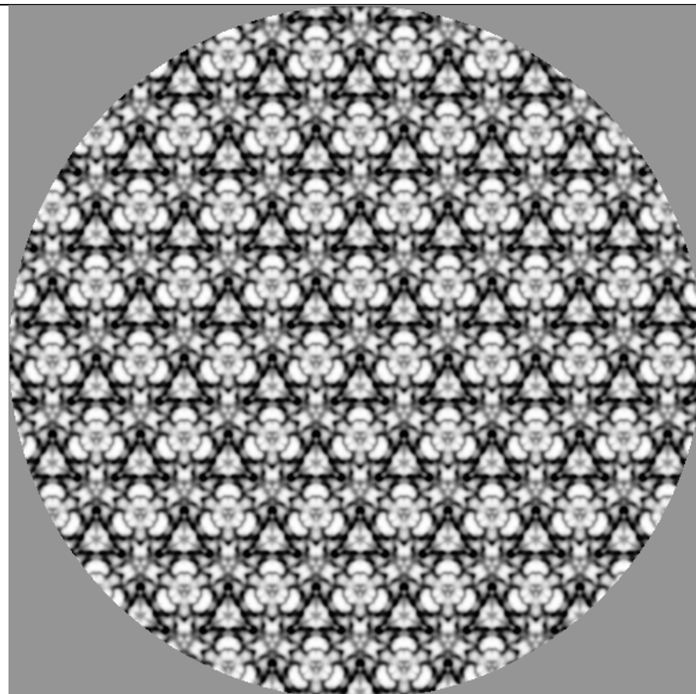	.1964
(b)	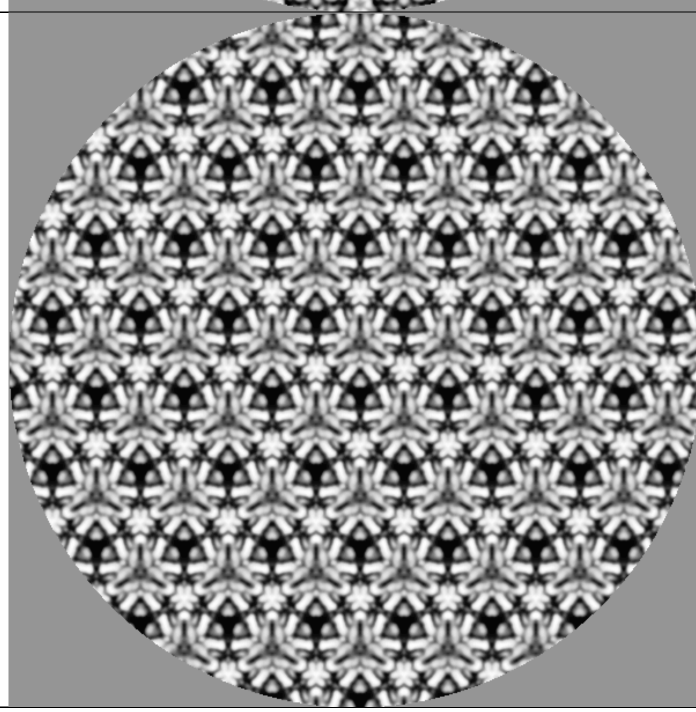	0.1249

Figure C-2. P3M1. (a) Exemplar with highest mean Jaccard index. (b) Exemplar with lowest mean Jaccard index.

	P31M Exemplars	Mean Jaccard index
(a)	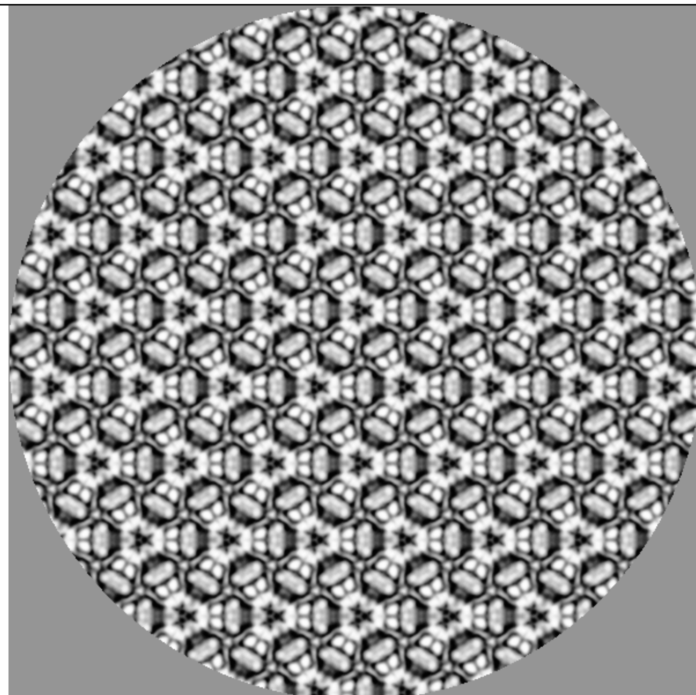	.1964
(b)	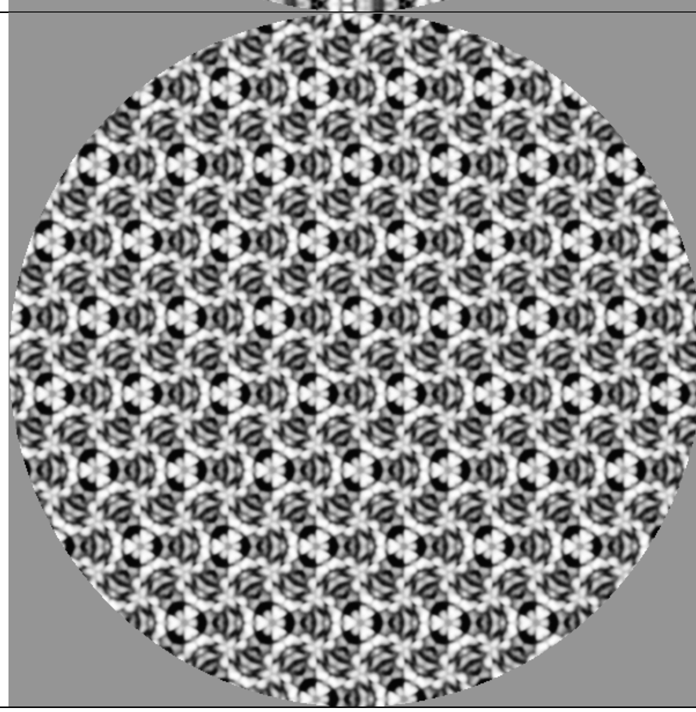	0.1100

Figure C-3. P31M. (a) Exemplar with highest mean Jaccard index. (b) Exemplar with lowest mean Jaccard index.

	P6 Exemplars	Mean Jaccard index
(a)	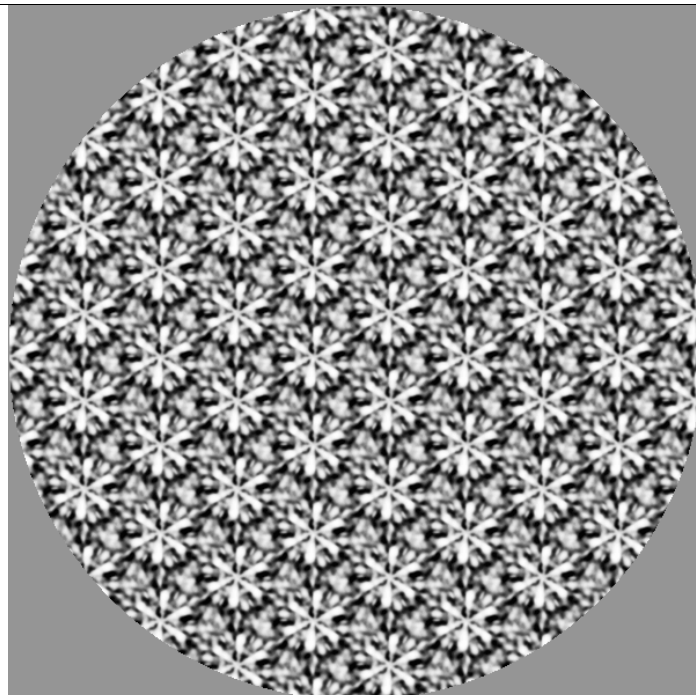	.1488
(b)	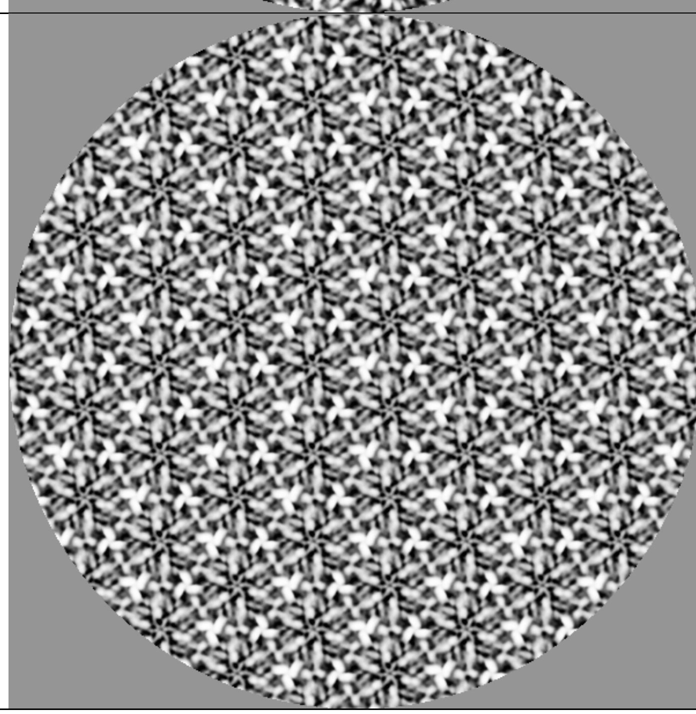	0.0884

Figure C-4. P6. (a) Exemplar with highest mean Jaccard index. (b) Exemplar with lowest mean Jaccard index

	P6M Exemplars	Mean Jaccard index
(a)	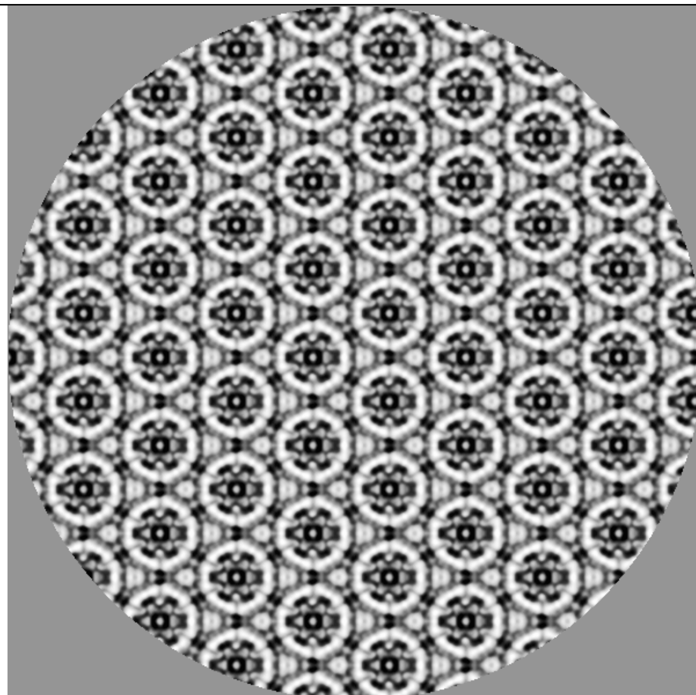	.2166
(b)	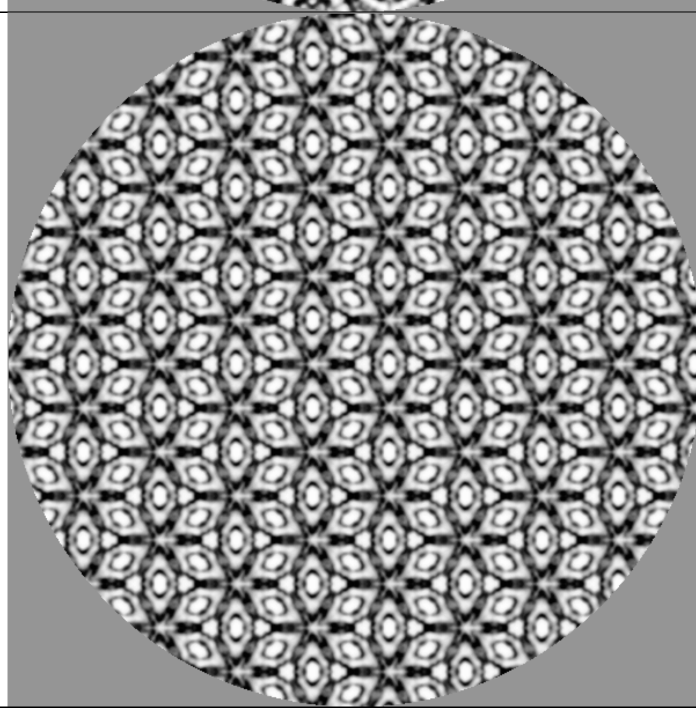	0.1076

Figure C-5. P6M. (a) Exemplar with highest mean Jaccard index. (b) Exemplar with lowest mean Jaccard index

BIBLIOGRAPHY

Capra, M. G. (2005). Factor Analysis of Card Sort Data: An Alternative to Hierarchical Cluster Analysis. *Proceedings of the Human Factors and Ergonomics Society Annual Meeting*, *49*(5), 691–695. doi:10.1177/154193120504900512

Clarke, A. D. F., Green, P. R., Halley, F., & Chantler, M. J. (2011). Similar Symmetries: The Role of Wallpaper Groups in Perceptual Texture Similarity. *Symmetry*, *3*(4), 246–264. doi:10.3390/sym3020246

Julesz, B. (2006). *Foundations of cyclopean perception* (1st MIT Press ed.). Cambridge, Mass: MIT Press.

Nucci, M., & Wagemans, J. (2007). Goodness of regularity in dot patterns: global symmetry, local symmetry, and their interactions. *Perception*, *36*(9), 1305–1319. doi:10.1068/p5794

Park, M., Lee, S., Chen, P.-C., Kashyap, S., Butt, A. A., & Liu, Y. (2008). Performance evaluation of state-of-the-art discrete symmetry detection algorithms. In *IEEE Conference on Computer Vision and Pattern Recognition, 2008. CVPR 2008* (pp. 1–8). doi:10.1109/CVPR.2008.4587824

Schattschneider, D. (1978). The Plane Symmetry Groups: Their Recognition and Notation. *The American Mathematical Monthly*, *85*(6), 439–450. doi:10.2307/2320063

Swaddle, J. P. (1999). Visual signaling by asymmetry: a review of perceptual processes. *Philosophical Transactions of the Royal Society of London. Series B: Biological Sciences*, *354*(1388), 1383–1393.

Treder, M. S. (2010). Behind the Looking-Glass: A Review on Human Symmetry Perception. *Symmetry*, *2*(3), 1510–1543. doi:10.3390/sym2031510

Tyler, C. W. (1995). Empirical aspects of symmetry perception. *Spatial Vision*, *9*(1), 1–8.

Tyler, C. W. (2000). The human expression of symmetry: art and neuroscience. In *ICUS Symmetry Symposium, Seoul*.

Wenderoth, P. (1996). The Effects of Dot Pattern Parameters and Constraints on the Relative Salience of Vertical Bilateral Symmetry. *Vision Research*, *36*(15), 2311–2320. doi:10.1016/0042-6989(95)00252-9

Weyl, H. (1952). *Symmetry*. Princeton: Princeton University Press.

Zhang, L., & Gerbino, W. (1992). Symmetry in opposite-contrast dot patterns. *Perception*, *21*(suppl 2), 95.

ACADEMIC VITA

Shivam Vedak
shivam.vedak@gmail.com

EDUCATION

High School Diploma
Illinois Math & Science Academy, Aurora, IL
Graduation: May 2010
Senior Thesis: Modeling Thermal Pain Perception

PROFESSIONAL EXPERIENCE

Research Assistant, Gilmore Brain Development Lab **2010 - Present**
The Pennsylvania State University, University Park, PA
- Currently researching the neural development of complex vision in humans using EEG and fMRI
- Honors thesis was completed within this lab

Physician Shadowing, Centegra Sage Cancer Center **Summer 2013**
Centegra Health System, McHenry, IL
- Experience shadowing medical and radiation oncologists through patient visits, treatment sessions, and board meetings
- Gained understanding of the multidisciplinary approach inherent to treatment within the field of oncology, including dosimetry and medical physics

Research Assistant, Apkarian Pain and Passions Lab **2008-2010**
Northwestern University, Feinberg School of Medicine, Chicago, IL
- Investigated the neural processes underlying pain perception in both humans and rats primarily focusing on the mechanisms of thermal pain perception

Summer Intern, Bloom Mind and Development Lab **Summer 2011**
Yale University, New Haven, CT
- Investigated the development of fairness concerns in children, as well as the nature of objectification in adults
- Led to publication of Sheskin, M., Bloom, P., & Wynn, K. (2014). Anti-equality: Social comparison in young children. *Cognition*, *130*(2), 152–156. doi:10.1016/j.cognition.2013.10.008
- Led to the publication of Gray, K., Knobe, J., Sheskin, M., Bloom, P., & Barrett, L. F. (2011). More than a body: Mind perception and the nature of objectification. *Journal of Personality and Social Psychology*, *101*(6), 1207–1220. doi:10.1037/a0025883

HONORS

Phi Beta Kappa Honor Society Member **2014-Present**
Pennsylvania State University Lambda Chapter

Psi Chi Psychology Honor Society Member **2014-Present**
Pennsylvania State University Chapter

Alpha Epsilon Delta Premedical Honor Society Member **2012-Present**
Pennsylvania Beta Chapter

1st Place in Social & Behavioral Sciences **2011**
Penn State Undergraduate Research Exhibition

- Received award for poster presentation on the steady-state visual evoked potentials (ssVEPs) of adults in response to various optic flow patterns, measured through a 128-channel EEG net

POSTERS & PRESENTATIONS

Penn State Undergraduate Research Exhibition **2012**
The Pennsylvania State University, University Park, PA
Vedak, S., Gonzalez, L., Mancino, A. *The Tuning of Child Brain Responses to Optic Flow*.

Penn State Undergraduate Research Exhibition **2011**
The Pennsylvania State University, University Park, PA
Vedak, S., Groner, R., Mancino, A. *Differential Adult Responses to Various Patterns of Optic Flow.*

IMSAloquium **2010**
The Illinois Mathematics & Science Academy, Aurora, IL
Vedak, S. Apkarian, A. V. *Modeling Thermal Pain Perception*